



**NRF**  
National Research  
Foundation

**SARAO**

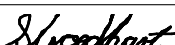
South African Radio  
Astronomy Observatory

<b>Organisation:</b>	NRF (National Research Foundation)
<b>Facility:</b>	SARAO (South African Radio Astronomy Observatory)
<b>Project:</b>	MeerKAT
<b>Type:</b>	Commissioning Test

## **Beamformer Coherency Commissioning Tests in 1K-mode at L-band**

<b>Document number:</b>	M2600-0000-042
<b>Revision:</b>	1
<b>Classification:</b>	Public
<b>Author:</b>	M. Geyer, S. Buchner, M. Serylak
<b>Date:</b>	2 February 2021

## Document Approval

	Name	Designation	Affiliation	Signature/Date
Submitted by	M. Geyer	Jnr Commissioning Scientist	SARAO	 M. Geyer
Reviewed by	M. Serylak	Commissioning Scientist	SARAO	 Maciej Serylak
Approved by	S. Goedhart	Manager: Commissioning	SARAO	 S. Goedhart Sharmila Goedhart (Feb 8, 2021 13:24 GMT+2)

## Document History

Revision	Date of Issue	Person Responsible	Comments
A	Sep 2019	M. Geyer	First draft

## Document Software

	Package	Version	Filename
Stylesheet	katscidoc	2.0	katscidoc.sty
Word processor	Overleaf	2.0	

## Organisation Details

Name	SARAO, Cape Town Office (Pinelands, Western Cape)	SARAO, Johannesburg Office (Rosebank, Gauteng)
Physical/Postal Address	Black River Park 2 Fir Street Observatory Cape Town 7925 South Africa	1st Floor 17 Baker Street Rosebank Gauteng 2196 South Africa
Tel.	+27 (0) 21 531 7282	+27 (0) 11 268 3400
Fax	+27 (0) 21 531 9761	+27 (0) 11 442 2454
Website	<a href="http://www.ska.ac.za">http://www.ska.ac.za</a>	<a href="http://www.ska.ac.za">http://www.ska.ac.za</a>

## Contents

<b>1</b>	<b>Introduction</b>	<b>5</b>
1.1	Purpose and Scope . . . . .	5
<b>2</b>	<b>Observational Procedure</b>	<b>5</b>
2.1	Prerequisites . . . . .	5
2.1.1	An initialized active array . . . . .	5
2.1.2	Delay calibration . . . . .	6
2.1.3	Phased-up array . . . . .	6
2.2	Observing software . . . . .	6
2.2.1	Multiple Schedule Blocks . . . . .	6
2.2.2	Single Schedule block . . . . .	7
2.3	Target selection . . . . .	7
2.4	Duration . . . . .	7
<b>3</b>	<b>Analysis method</b>	<b>8</b>
3.1	Reductional software . . . . .	8
3.2	Test metrics and verification . . . . .	9
<b>4</b>	<b>Data Analysis</b>	<b>9</b>
4.1	Data summary . . . . .	9
4.2	RFI excision . . . . .	9
4.3	Coherency estimates . . . . .	9
<b>5</b>	<b>Results</b>	<b>14</b>
<b>6</b>	<b>Next steps and remarks</b>	<b>14</b>
<b>7</b>	<b>Acknowledgements</b>	<b>15</b>
<b>A</b>	<b>Appendix A: Data Summary</b>	<b>15</b>
A.1	Tied-Array Beam coherency commissioning data . . . . .	15
A.2	Associated phase-up information . . . . .	24

## List of Figures

- |   |                                                                                                                                                                                                                                                                                                                                                                                                                                                                                                                                                                                                                                                                                                                                              |    |
|---|----------------------------------------------------------------------------------------------------------------------------------------------------------------------------------------------------------------------------------------------------------------------------------------------------------------------------------------------------------------------------------------------------------------------------------------------------------------------------------------------------------------------------------------------------------------------------------------------------------------------------------------------------------------------------------------------------------------------------------------------|----|
| 1 | Plots presenting the (normalised) S/N obtained for PSR J1056–6258 against the number of antennas present in the array to showcase the coherency achieved with the full MeerKAT array in 1K mode. Issues with particular antennas or schedule blocks per coherency test are captured in Table 2 and particular scans accordingly removed. . . . .                                                                                                                                                                                                                                                                                                                                                                                             | 11 |
| 2 | Coherency achieved on PSR J1056–6258 with the full MeerKAT array in 1K continued. . . . .                                                                                                                                                                                                                                                                                                                                                                                                                                                                                                                                                                                                                                                    | 12 |
| 3 | Similar to Fig. 1 we present the coherency achieved on PSR J1644–4559 with the full MeerKAT array in 1K mode. As described in Sec. 5 the average coherency factor achieved on PSR J1644–4559 is somewhat lower than on PSR J1056–6258. . . . .                                                                                                                                                                                                                                                                                                                                                                                                                                                                                               | 13 |
| 4 | Average coherency values across 19 sets of coherency test observations in 1K mode. Results are obtained using 200 mostly RFI clean frequency channels (blue circles), and further improved upon by additional cleaning via the COAST GUARD (CG) cleaning algorithm (red squares). The mean power law index values ( $\alpha$ ) obtained across these observations are $\langle \alpha \rangle = 0.98 \pm 0.02$ (blue dashed line) and $\langle \alpha_{CG} \rangle = 0.99 \pm 0.01$ (red solid line) respectively. As discussed the flux density of PSR J1056–6258 provides a better target for these tests. Using only data from observations of this pulsar we achieve a minimum $\alpha$ value of $0.95 \pm 0.03$ (solid green line). . . | 13 |

## List of Tables

- |   |                                                                                                                                                                                                                                                                                                                         |    |
|---|-------------------------------------------------------------------------------------------------------------------------------------------------------------------------------------------------------------------------------------------------------------------------------------------------------------------------|----|
| 1 | An overview of the relevant target pulsar parameters. Flux density values are taken from the <i>psrcat</i> catalog as referenced in the text. . . . .                                                                                                                                                                   | 8  |
| 2 | Overview of coherency tests run on PSRs J1056–6258 and J1644–4559, along with known issues and comments. . . . .                                                                                                                                                                                                        | 10 |
| 3 | An overview of obtained coherency indices ( $\alpha$ ) and their measured $1\sigma$ standard deviations ( $\sigma_\alpha$ ) over the full set of experiments. Coherency values and standard deviations obtained by running additional RFI reduction using the COAST GUARD software are labelled with CG subscripts. . . | 14 |
| 4 | Tied-Array Beam 1K data of pulsars J1056–6258 and J1644–4559 recorded using the PTUSe backend between March 2019 and September 2019 for beam coherency tests, labelled here as Experiments 1 to 20. . . . .                                                                                                             | 15 |
| 5 | Summary of the phase-up schedule blocks and targets associated with the set of experiments run.                                                                                                                                                                                                                         | 24 |

## List of Abbreviations

TAB	Tied-Array Beam
PTUSe	Pulsar User Supplied Equipment
CAM	Control and Monitoring
RFI	Radio Frequency Interference
SDP	Science Data Processing
SKA	Square Kilometer Array
SKARAB	SKA Reconfigurable Application Board

# 1 Introduction

Similar to an earlier commissioning report (M2600-0000-010) on the coherency of the MeerKAT Tied-Array Beam (TAB) in the 4096 frequency channel (4K) mode, this report investigates the level of coherency of the TAB in the 1024 frequency channel (1K) mode at L-band frequencies (856 MHz to 1712 MHz). The 1K-mode is designed specifically for high precision pulsar timing work, exchanging frequency resolution for higher timing resolution, and is the preferred mode for most Meertime<sup>1</sup> pulsar observations.

In the 1K folded mode used here, the Pulsar Timing User Supplied Equipment (PTUSE) provides 8 second folded profiles, with 1024 phase bins per profile, similar to the 4K folded mode.

The data quality of the TAB is monitored while observing a well-known pulsar and changing the number of antennas used to form the TAB. The signal-to-noise-ratio (S/N) of the pulsar observation is expected to increase linearly with an increasing number of antennas. Perfect antenna addition would produce a coherency value ( $\alpha$ ) of 1.0.

The primary target used for these tests is PSR J1056–6258, as per the 4K report (M2600-0000-010), along with a couple of observations using PSR J1644–4559.

The TAB coherency specification is described in R.C.SP.23 CBF TA beamforming efficiency as follows: "*The Correlator Beamformer (CBF), when requested to produce one or more TA beams, shall maintain, with an efficiency factor of  $>= 0.95$ , constant S/N per TA produced.*"

We find that this specification is met by achieving a mean coherency factor of  $\langle \alpha \rangle = 0.99 \pm 0.01$  and a minimum  $\alpha$  value using PSR J1056–6258 of  $0.95 \pm 0.03$ .

## 1.1 Purpose and Scope

The purpose of this report is to investigate the coherency of the TAB using the L-band receivers (856 MHz to 1712 MHz) in a large array, i.e with the 64-antenna correlator, in its 1K mode (1024 frequency channels). Within the scope of this test lies understanding where deviations from expected trends could arise from, as well as investigating whether TAB coherency is consistently achieved. This means these tests have to be repeated, sampling different antenna sets.

Achieving a coherent result for the TAB through pulsar data analysis relies on,

- ensuring a successful delay calibration and phased-up array before observing pulsar targets;
- effectively removing RFI from the data, which greatly impacts pulsar S/N estimates.

# 2 Observational Procedure

## 2.1 Prerequisites

The following are observing and calibration prerequisites for conducting effective TAB coherency tests.

### 2.1.1 An initialized active array

A large array (antennas  $\gtrsim 50$ ) built to include control resources ptuse\_1 or ptuse\_2, the (current) user supplied pulsar backend machines in bc856M1k correlator mode. This mode records the full MeerKAT L-band (bandwidth of 856 MHz) with 1024 frequency channels and dual polarisation as 8 second folded pulsar archive files.

<sup>1</sup>[www.meertime.org](http://www.meertime.org)

### 2.1.2 Delay calibration

A standard 1K delay calibration needs to be performed on the activated array. The delay calibration procedure firstly applies pre-defined F-engine gain values and thereafter, following a short observation of a well-known calibrator and the noise diode, corrects for geometrical delays between antennas ( $K$ ), as well as delays between polarisations ( $K_{Cross}$ ).

### 2.1.3 Phased-up array

After successful delay calibration a so-called ‘flatten bandpass phase-up’ is required. During the phase-up procedure a well-known calibrator source and the noise diode are observed again, and the delay products above,  $K$  and  $K_{Cross}$ , are re-derived such that finer improvements to the original delay solutions are obtained. In addition bandpass correction (or flattening) is applied ( $B$ ) as well as a complex gain solution for each antenna ( $G$ )<sup>2</sup>. Following the application of this full set of calibration solutions the F-Engine data are added in phase in the B-Engine to form the TAB data stream. The array is now in a ‘phased-up’ state on which coherency tests can be executed.

## 2.2 Observing software

During these observations two different softwares were developed to investigate the coherency of the TAB. An initial *multi schedule block* method which conveniently creates a single data archive entry for every configuration (number of antennas) that was used during the observation. This however increases the combined overheads of the commissioning observation, since many schedule blocks need to be executed. To streamline the observing time a *single schedule block* script was developed which creates a single archive data entry for the commissioning test.

### 2.2.1 Multiple Schedule Blocks

The observation is started by executing `python make_TAB_SB.py` on the observation machine in `usersnfs/mgeyer`. This script checks which antennas are in the active subarray and (excluding antennas which were marked faulty by operators) produces and unloads a set of schedule blocks onto the CAM GUI for the operator to run.

Arguments to this script are set as follows,

```
optional arguments:
  -h, --help            show this help message and exit
  -o <observer_name>, --observer <observer_name>
                        specify observer name (default = Marisa)
  -pid <proposal_id>, --prop_id <proposal_id>
                        specify proposal id (default = COM-20180614-MG-01)
  -t <target_name>, --target <target_name>
                        specify target (default = J1056-6258)
  -dscrpt <description_str>, --description <description_str>
                        specify schedule block description (default =
                        COM-20180614-MG-01 1K TAB coherency)
  -time <target_time>, --time <target_time>
                        specify time (sec) on target per observation (default
                        = 300)
  -drop <nants_drop>, --drop <nants_drop>
                        specify number of antennas to change between
                        configurations (default = 3)
```

<sup>2</sup>In later versions of the calibration pipeline (after April 2020) corrections to the polarisation phase offsets ( $BCross\_Sky$ ) are also applied during the phase-up procedure

The observing script that will be executed, as called from the created schedule blocks is *beamform\_single.py* from the [katusescripts GitHub repository](#). In each SB the generated -nants list is changed to create arrays of independent sizes. Each configuration (in other words array with a specific number of antennas) is run as an independent SBs. Example schedule blocks and supporting documentation can be found [here](#).

The advantage of this script generating individual schedule blocks was that it guaranteed the number of antennas for a given observing configuration, such that there was no ambiguity in terms of whether for example antenna weights were changed correctly from one configuration to a next or analysing when the weight changes occurred. It also allowed the observations to be easily used as fillers within the MeerKAT schedule, since operations could load a maximum number of short schedule blocks (e.g 20), but could opt to only run a smaller number if other scheduling constraints arose.

### 2.2.2 Single Schedule block

Observations from August 2019 onwards were run using a different script based on *beamform\_multi.py*, namely *beamform\_coherency.py*. This script makes use of the optimisations of the *beamform\_multi.py* which minimises time between observations on different targets. In the case of *beamform\_coherency.py* the time it took to switch between antennas configurations (by setting antennas weights) was therefore optimised w.r.t the multi schedule block method. Antenna weights were set similar to as described in the 4K report (M2600-0000-010). These scripts are all within the [katusescripts GitHub repository](#). Running *beamformer\_coherency.py* results in single entries in the SARAO archive, but still produces independent observing folders via PTUSE for each configuration on one of the PTUSE machines.

Antennas were typically removed from largest numbered names to smallest - which roughly corresponds to removing the outer ring antennas first, and the core antennas last.

### 2.3 Target selection

Observations are conducted on PSR J1644–4559 and J1056–6258, two bright pulsars. Both are normal (i.e. slow) pulsars with periods between 0.4 and 0.5 seconds.

Their high Southerly declination values mean that they are observable to MeerKAT for more than 12 hrs a day, allowing ease of scheduling of the coherency test experiments.

An overview of the relevant pulsar parameters are given in Table 1. Both pulsars are known to be flux stable and due to their high dispersion measure (DM) values are non-scintillating, making them ideal test candidates. The flux values presented are the S<sub>1400</sub> flux estimates at 1400 MHz from the *psrcat*<sup>3</sup> catalog.

As described in the 4K-report (M2600-0000-010) a concern that the peak flux of PSR J1644–4559 is too high, and therefore contributing to the system temperature lead to an increase usage of PSR J1056–6258 for these tests.

### 2.4 Duration

A typical observation spends approximately 300 seconds in a given antenna configuration and cycles through 15 to 30 configurations per observation, such that the total observing duration is ~1 - 2.5 hours. Added to this is the time to build the subarray as well as a delay calibration (~10 min) and a successful phase-up (~15 min). The number of antennas removed between configurations typically vary between 2 and 4 (most often using 3), to sample the array effectively.

<sup>3</sup>[www.atnf.csiro.au/people/pulsar/psrcat](http://www.atnf.csiro.au/people/pulsar/psrcat)

Table 1: An overview of the relevant target pulsar parameters. Flux density values are taken from the *psrcat* catalog as referenced in the text.

Target pulsar	Pulse period (s)	DM (pc cm <sup>-3</sup> )	Catalog S <sub>1400</sub> flux values (mJy)
J1644–4559	0.455	478.8	296.4
J1056–6258	0.422	320.3	34.0

### 3 Analysis method

The data are captured using the PTUSE pipeline, which means 8s integrations are saved to one of the PTUSE machines (formerly ‘kronos’ machines). From here data are ingested to both our archive<sup>4</sup> as well as the Ozstar supercomputer at Swinburne University of Technology in Melbourne.

Supporting visibility data (fdb-files) are downloaded from the archive to check associated metadata. In particular the fdb-file associated with the phase-up observation is required to check whether the array was effectively phased-up. The success of the outcome of this experiment relies on a successful phase-up. All observations included to this report have been checked for good phase-up results via the SDP calibration reports, as well as Maciej Serylak’s phase-up notebook (see <https://github.com/ska-sa/katpulse>).

#### 3.1 Reductional software

The pulsar data are analysed using a software procedure (*reduce\_TAB.py*) developed for the purpose hosted in [katpulse](#) in the commissioning directories.

The analysis relies on some standard pulsar software implementations mainly based on PSRCHIVE<sup>5</sup> tools:

- `psradd` (module within PSRCHIVE) is used to add 8 second integrations to form a single added observation per configuration
- `paz` (module within PSRCHIVE) is used to remove all but 200 frequency channels
- `pam` (module within PSRCHIVE) with flags `-DFTp` is run to create single average pulsar profiles (dedispersed, frequency, time and polarisation integrated)
- surgical `clean.py` from the COAST GUARD package is run on the 200 selected channels for additional RFI excision
- the signal-to-noise ratio (S/N) of the remaining average pulse profile shapes are computed using `psredit` (module within PSRCHIVE) with flags `-c snr=snr, pdmp`
- the computed S/N values are plotted against number of antennas for each configuration, after which a power law is fit through the S/N vs N<sub>ants</sub> data. This is done using the `lmfit` library within PYTHON.

<sup>4</sup>The procedure for this is currently changing so that ultimately pulsar data will also reach the archive via an automatic ingest to the CEPH cluster at the CHPC

<sup>5</sup><http://psrchive.sourceforge.net/>

### 3.2 Test metrics and verification

The test metric for coherency is a power-law exponent when fitting data points of pulsar S/N values against number of antennas in the TAB. Perfect coherent addition would lead to a power-law exponent (or here a coherency value) of 1.0. As described in the introduction, the MeerKAT SKARAB correlator is specified to reach a coherency value  $\alpha$  of  $\alpha > 0.95$ .

## 4 Data Analysis

### 4.1 Data summary

A full log of the data run for 1K TAB experiments from March 2019 to September 2019 is documented in Appendix A1 in Table 4. Details of the associate phase-up observations for each of these coherency experiments are captured in Table 5 in Appendix A2. All data were run under the proposal ID: COM-20180614-MG-01.

For ease of analysis and discussion here, the data are labelled as Experiments 1 - 20. Experiments 1 - 17 were run using multiple schedule blocks and running *beamformer\_single.py* as described above in Section 2.2, while Experiments 18 to 20 were run using *beamformer\_coherency.py* based on *beamformer\_multi.py* which results in a single entry per observation in the SARAO archive, but still produces independent observing folders on one of the PTUSe machines. An overview of the experiments including issues related to individual observations are in Table 2.

All data that were obtained under the COM-20180614-MG-01 proposal ID are included in this report.

### 4.2 RFI excision

The standard RFI excision procedure for these experiments are aimed at being highly conservative: i.e. only a small number of channels known to be mostly free of RFI is retained, and most others removed. Since the pulsars are bright we pick to use only 200 channels of RFI-clean frequency channels in 1K mode, namely channels 540 to 740 corresponding to frequencies 1306 MHz to 1474 MHz. The HI-line at 1412 MHz lies within this range and is additionally removed.

After selecting these 200 frequency channels we perform additional RFI excision by using the COAST GUARD package. The software within this package that we run is called *clean.py* and is run by using it in its ‘surgical cleaner’ mode. A similar procedure was followed for the 4K experiments described in the 4K commissioning report (M2600-0000-010).

### 4.3 Coherency estimates

Fitting a power law across a S/N vs number of antenna plot, we determine the level of coherency (and its associated uncertainty) of the TAB. A perfectly coherent beam would produce a linear dependence on S/N with number of antennas, i.e. a power-law with exponent  $\alpha = 1$ . Figs. 1 and 2 show the results for all experiments observing PSR J1056–6258, and Fig. 3 shows the results on PSR J1644–4559. A fit of the form  $S/N = A * N_{\text{ants}}^{\alpha} + c$  is computed for the S/N values estimated from both the ‘200 channels only’ data sets and the ‘200 channels only’ data sets with additional COAST GUARD (CG) cleaning of RFI.

Table 2: Overview of coherency tests run on PSRs J1056–6258 and J1644–4559, along with known issues and comments.

Label	Date	Target	Max ants	scans	$\Delta$ ants	Multiple SBs	Comments
Exp 1	2019-03-20	J1056–6258	58	15	4	Y	
Exp 2	2019-04-03	J1056–6258	58	19	3	Y	First scan has antennas m039 and m054 that were marked faulty thereafter. Excluding first scan.
Exp 3	2019-04-04	J1056–6258	59	19	2	Y	Antennas m039 and m054 were noisy, but not marked faulty. Excluding all scans with these antennas.
Exp 4	2019-04-09	J1056–6258	52	18	3	Y	
Exp 5	2019-04-29	J1056–6258	57	22	3	Y	
Exp 6	2019-05-16	J1056–6258	60	21	3	Y	
Exp 7	2019-05-16	J1644–4559	60	21	3	Y	
Exp 8	2019-06-07	J1056–6258	62	13	3	Y	Observation interrupted for science.
Exp 9	2019-06-08	J1056–6258	62	18	3	Y	Antenna m057 had bad phase solutions; marked faulty after the first scan. Excluding first scan from analysis.
Exp 10	2019-06-16	J1056–6258	60	22	3	Y	Antenna m057 had bad phase solutions, removing scans which included m057.
Exp 11	2019-06-17	J1644–4559	59	22	3	Y	F-hosts disabled during observation, resulted in the data loss for one schedule block.
Exp 12	2019-07-11	J1056–6258	56	19	3	Y	
Exp 13	2019-07-21	J1056–6258	60	22	3	Y	
Exp 14	2019-08-02	J1644–4559	58	20	3	Y	
Exp 15	2019-08-03	J1056–6258	58	20	3	Y	Strong time domain RFI in Nants = 50, well treated by the COAST GUARD RFI cleaner.
Exp 16	2019-08-10	J1056–6258	61	21	3	Y	
Exp 17	2019-08-13	J1056–6258	18	3		Y	These are the last three scans of the multi schedule block execution. They are jointly analysed with Exp 18.
Exp 18	2019-08-13	J1056–6258	45	15	3	N	
Exp 19	2019-08-25	J1056–6258	60	21	3	N	Code bug: antennas were ‘dropped’ from the core outwards.
Exp 20	2019-09-01	J1056–6258	60	15	3	N	

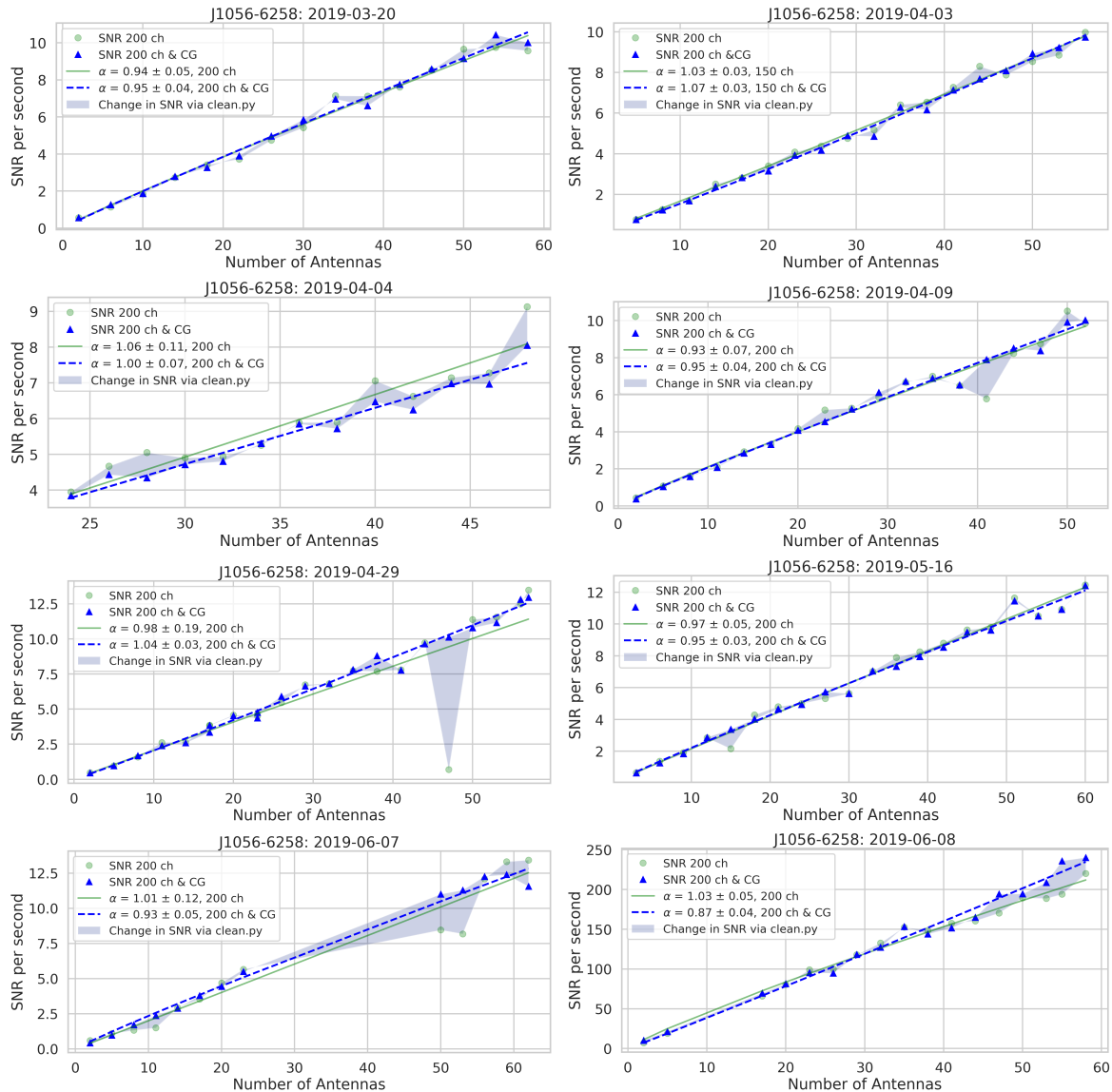


Figure 1: Plots presenting the (normalised) S/N obtained for PSR J1056–6258 against the number of antennas present in the array to showcase the coherency achieved with the full MeerKAT array in 1K mode. Issues with particular antennas or schedule blocks per coherency test are captured in Table 2 and particular scans accordingly removed.

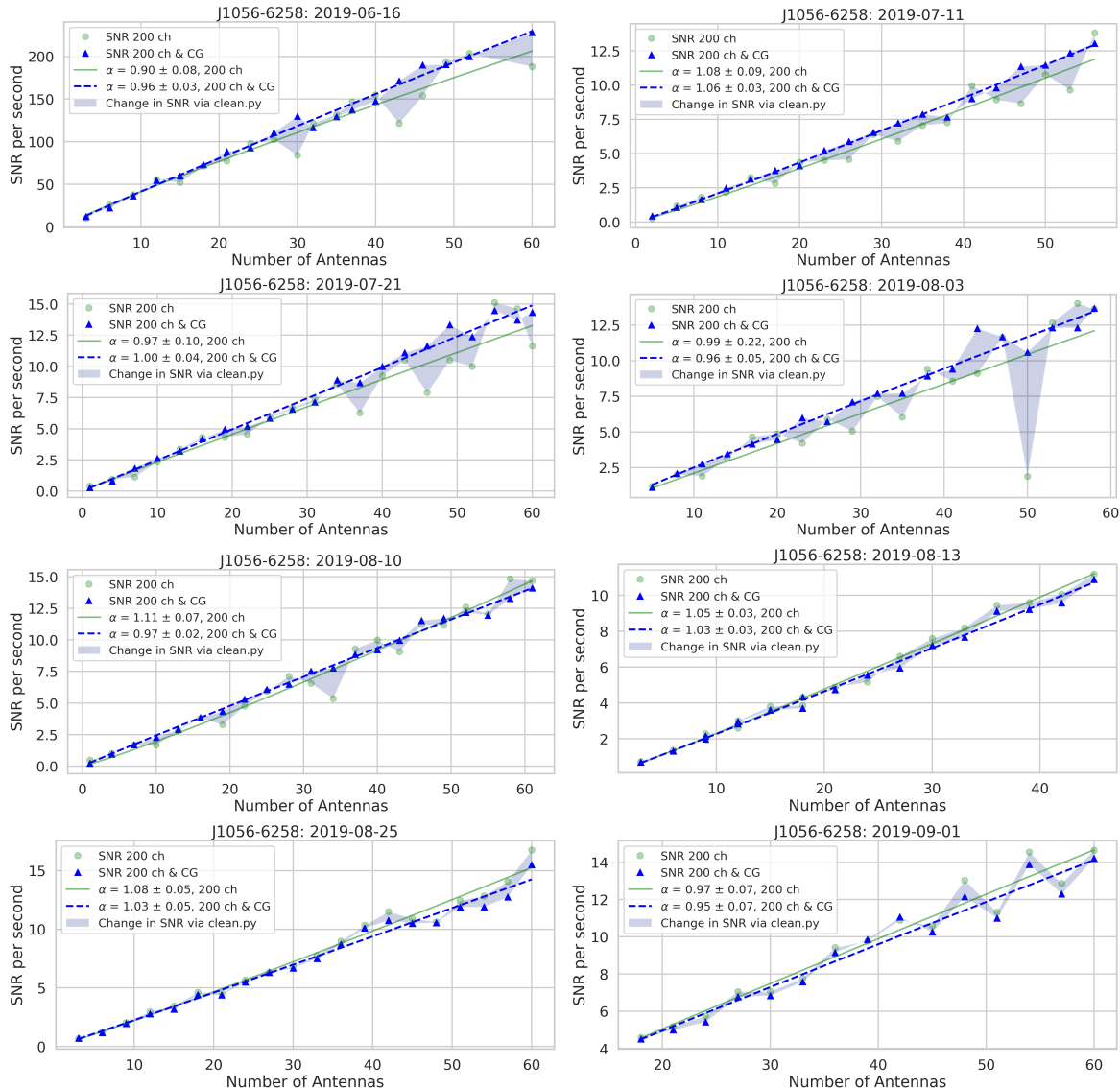


Figure 2: Coherency achieved on PSR J1056–6258 with the full MeerKAT array in 1K continued.

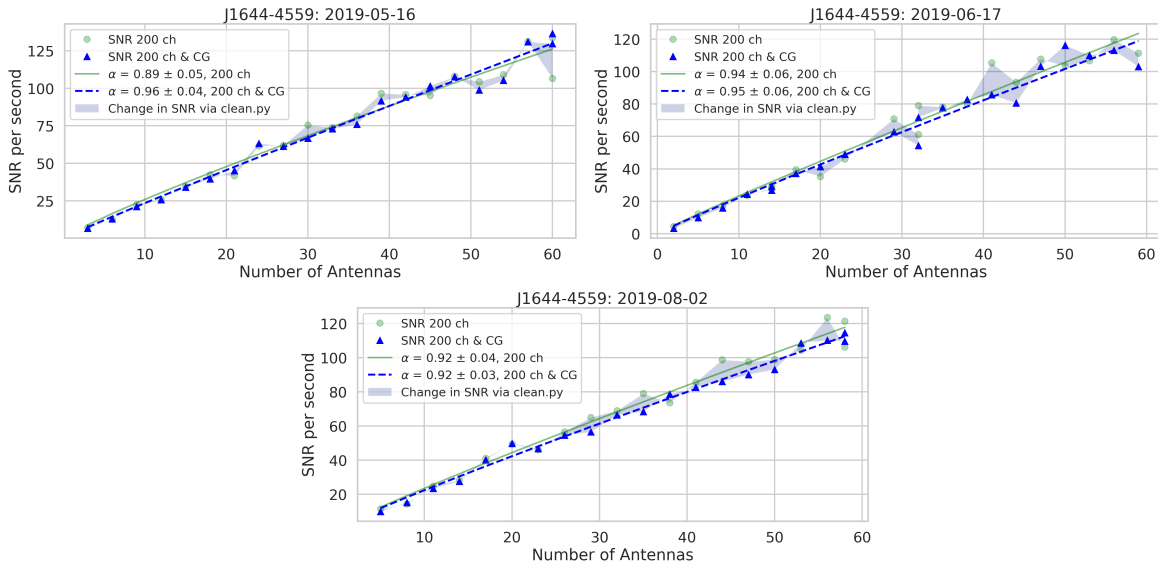


Figure 3: Similar to Fig. 1 we present the coherency achieved on PSR J1644–4559 with the full MeerKAT array in 1K mode. As described in Sec. 5 the average coherency factor achieved on PSR J1644–4559 is somewhat lower than on PSR J1056–6258.

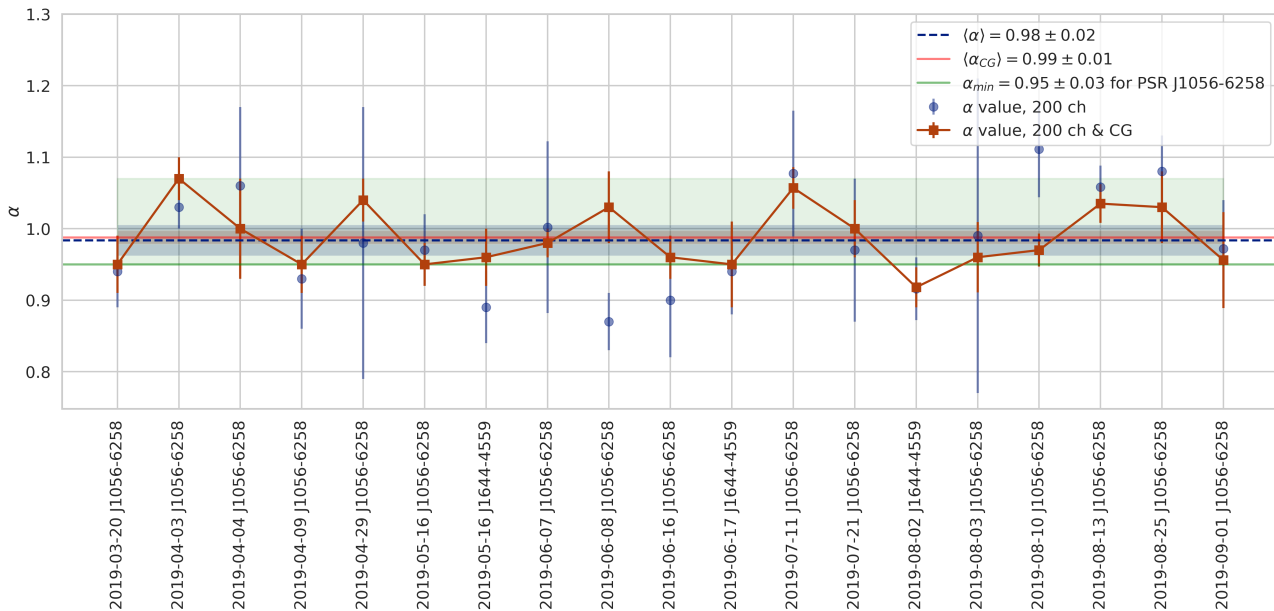


Figure 4: Average coherency values across 19 sets of coherency test observations in 1K mode. Results are obtained using 200 mostly RFI clean frequency channels (blue circles), and further improved upon by additional cleaning via the COAST GUARD (CG) cleaning algorithm (red squares). The mean power law index values ( $\alpha$ ) obtained across these observations are  $\langle \alpha \rangle = 0.98 \pm 0.02$  (blue dashed line) and  $\langle \alpha_{CG} \rangle = 0.99 \pm 0.01$  (red solid line) respectively. As discussed the flux density of PSR J1056–6258 provides a better target for these tests. Using only data from observations of this pulsar we achieve a minimum  $\alpha$  value of  $0.95 \pm 0.03$  (solid green line).

Label	Target	Date	$\alpha$	$\sigma_\alpha$	$\alpha_{CG}$	$\sigma_{\alpha CG}$
Exp1	J1056–6258	2019-03-20	0.94	0.05	0.95	0.04
Exp2	J1056–6258	2019-04-03	1.03	0.03	1.07	0.03
Exp3	J1056–6258	2019-04-04	1.06	0.11	1.00	0.07
Exp4	J1056–6258	2019-04-09	0.93	0.07	0.95	0.04
Exp5	J1056–6258	2019-04-29	0.98	0.19	1.04	0.03
Exp6	J1056–6258	2019-05-16	0.97	0.05	0.95	0.03
Exp7	J1644–4559	2019-05-16	0.89	0.05	0.96	0.04
Exp8	J1056–6258	2019-06-07	1.00	0.12	0.98	0.02
Exp9	J1056–6258	2019-06-08	0.87	0.04	1.03	0.05
Exp10	J1056–6258	2019-06-16	0.90	0.08	0.96	0.03
Exp11	J1644–4559	2019-06-17	0.94	0.06	0.95	0.06
Exp12	J1056–6258	2019-07-11	1.08	0.09	1.06	0.03
Exp13	J1056–6258	2019-07-21	0.97	0.10	1.00	0.04
Exp14	J1644–4559	2019-08-02	0.92	0.04	0.92	0.03
Exp15	J1056–6258	2019-08-03	0.99	0.22	0.96	0.05
Exp16	J1056–6258	2019-08-10	1.11	0.07	0.97	0.02
Exp17&18	J1056–6258	2019-08-13	1.06	0.03	1.03	0.03
Exp19	J1056–6258	2019-08-25	1.08	0.05	1.03	0.05
Exp20	J1056–6258	2019-09-01	0.97	0.07	0.96	0.07

Table 3: An overview of obtained coherency indices ( $\alpha$ ) and their measured  $1\sigma$  standard deviations ( $\sigma_\alpha$ ) over the full set of experiments. Coherency values and standard deviations obtained by running additional RFI reduction using the COAST GUARD software are labelled with CG subscripts.

## 5 Results

In this report we have found the coherency of the TAB in 1K mode to be within the required specifications ( $\alpha > 0.95$ ). This specification is achieved when a) a target source is picked for which the peak flux is not fractionally significant compared to the system temperature  $T_{sys}$  (see e.g. the 4K report, M2600-0000-010) and b) when a good phase-up of the array is achieved on a calibrator source.

Across the experiments analysed we obtain an overall average value of  $\langle \alpha \rangle = 0.98 \pm 0.02$  using 200 channels typically clean of RFI, and an improved  $\langle \alpha_{CG} \rangle = 0.99 \pm 0.01$  if we conduct further RFI excision on the data. As discussed in Sec. 2.3 on the choice of targets, we have found that the lower flux density of PSR J1056–6258 provides a better target for coherency tests over PSR J1644–4559. For the three J1644–4559 tests run we find  $\langle \alpha \rangle = 0.92 \pm 0.03$  and  $\langle \alpha_{CG} \rangle = 0.94 \pm 0.03$ , while averaged values on PSR J1056–6258 experiments are  $\langle \alpha \rangle = 0.996 \pm 0.025$  and  $\langle \alpha_{CG} \rangle = 0.996 \pm 0.010$ . Using only data from observations on PSR J1056–6258 we achieve a minimum  $\alpha$  value of  $0.95 \pm 0.03$ , fulfilling the requirement to have  $\alpha > 0.95$ .

## 6 Next steps and remarks

Next these tests will be conducted with the UHF receiver (operating at 544 - 1088 MHz) using 1024 channels. In particular efficient coherency at UHF can only be achieved if our UHF calibrator models match the accuracy of our L-band calibrator models used here, and if we correctly take into account the time scale over which we expect to be impacted by the ionosphere.

## 7 Acknowledgements

The authors thank members of the User Supplied Equipments (PTUSE, TUSE, FBFUSE and APUSE) for valuable discussions during the weekly telecon meeting.

## A Appendix A: Data Summary

### A.1 Tied-Array Beam coherency commissioning data

The following table captures the data information of all the TAB coherency tests run in 1K mode. Table 4 contains the starting time, schedule block identifier, associated number of antennas used during the observation and the captured duration for each configuration within each experiment run.

Table 4: Tied-Array Beam 1K data of pulsars J1056–6258 and J1644–4559 recorded using the PTUSE back-end between March 2019 and September 2019 for beam coherency tests, labelled here as Experiments 1 to 20.

#### *Experiment 1*

Start (UTC)	Schedule Block ID	Nants	Target	Duration (sec)
2019-03-20T17:28:32Z	20190320-0055	58	J1056–6258	600.00
2019-03-20T17:43:26Z	20190320-0060	54	J1056–6258	592.00
2019-03-20T17:57:51Z	20190320-0059	50	J1056–6258	592.00
2019-03-20T18:11:55Z	20190320-0058	46	J1056–6258	592.00
2019-03-20T18:27:22Z	20190320-0062	42	J1056–6258	592.00
2019-03-20T18:41:55Z	20190320-0061	38	J1056–6258	592.00
2019-03-20T18:56:24Z	20190320-0063	34	J1056–6258	599.04
2019-03-20T19:10:51Z	20190320-0064	30	J1056–6258	592.00
2019-03-20T19:25:44Z	20190320-0065	26	J1056–6258	592.00
2019-03-20T19:40:53Z	20190320-0068	22	J1056–6258	592.00
2019-03-20T19:55:24Z	20190320-0067	18	J1056–6258	592.00
2019-03-20T20:09:48Z	20190320-0066	14	J1056–6258	592.00
2019-03-20T20:27:15Z	20190320-0054	10	J1056–6258	592.00
2019-03-20T20:40:48Z	20190320-0070	6	J1056–6258	592.00
2019-03-20T20:56:20Z	20190320-0072	2	J1056–6258	592.00

#### *Experiment 2*

Start (UTC)	Schedule Block ID	Nants	Target	Duration (sec)
2019-04-03T22:46:48Z	20190403-0059	58	J1056–6258	296.00
2019-04-03T23:01:05Z	20190403-0060	56	J1056–6258	296.00
2019-04-03T23:09:41Z	20190403-0061	53	J1056–6258	295.19
2019-04-03T23:18:35Z	20190403-0063	50	J1056–6258	296.00
2019-04-03T23:26:42Z	20190403-0064	47	J1056–6258	288.00
2019-04-03T23:36:46Z	20190403-0066	44	J1056–6258	296.00
2019-04-03T23:44:50Z	20190403-0070	41	J1056–6258	288.00
2019-04-03T23:52:28Z	20190403-0068	38	J1056–6258	296.00
2019-04-04T00:00:03Z	20190403-0071	35	J1056–6258	295.96
2019-04-04T00:07:50Z	20190404-0001	32	J1056–6258	296.00
2019-04-04T00:15:19Z	20190404-0002	29	J1056–6258	296.00
2019-04-04T00:22:51Z	20190404-0003	26	J1056–6258	296.00
2019-04-04T00:30:22Z	20190404-0004	23	J1056–6258	296.00
2019-04-04T00:37:53Z	20190404-0005	20	J1056–6258	296.00
2019-04-04T00:45:33Z	20190404-0006	17	J1056–6258	288.00

2019-04-04T00:53:05Z	20190404-0007	14	J1056–6258	296.00
2019-04-04T01:01:01Z	20190404-0008	11	J1056–6258	296.00
2019-04-04T01:08:22Z	20190404-0009	8	J1056–6258	296.00
2019-04-04T01:18:28Z	20190404-0010	5	J1056–6258	295.23

*Experiment 3*

Start (UTC)	Schedule Block ID	Nants	Target	Duration (sec)
2019-04-04T22:35:28Z	20190404-0057	59	J1056–6258	296.00
2019-04-04T22:45:34Z	20190404-0058	58	J1056–6258	296.00
2019-04-04T22:53:46Z	20190404-0059	56	J1056–6258	296.00
2019-04-04T23:02:19Z	20190404-0060	54	J1056–6258	296.00
2019-04-04T23:09:56Z	20190404-0061	52	J1056–6258	296.00
2019-04-04T23:17:42Z	20190404-0062	50	J1056–6258	296.00
2019-04-04T23:29:33Z	20190404-0063	48	J1056–6258	296.00
2019-04-04T23:36:57Z	20190404-0064	46	J1056–6258	296.00
2019-04-04T23:45:00Z	20190404-0065	44	J1056–6258	296.00
2019-04-04T23:52:51Z	20190404-0066	42	J1056–6258	296.00
2019-04-05T00:00:54Z	20190404-0067	40	J1056–6258	288.00
2019-04-05T00:09:33Z	20190404-0068	38	J1056–6258	296.00
2019-04-05T00:17:26Z	20190404-0069	36	J1056–6258	296.00
2019-04-05T00:24:59Z	20190404-0070	34	J1056–6258	296.00
2019-04-05T00:32:50Z	20190404-0071	32	J1056–6258	295.73
2019-04-05T00:40:25Z	20190404-0072	30	J1056–6258	288.00
2019-04-05T00:48:16Z	20190405-0001	28	J1056–6258	288.00
2019-04-05T00:55:45Z	20190405-0002	26	J1056–6258	295.41
2019-04-05T01:03:50Z	20190405-0003	24	J1056–6258	288.00

*Experiment 4*

Start (UTC)	Schedule Block ID	Nants	Target	Duration (sec)
2019-04-09T14:57:44Z	20190409-0050	52	J1056–6258	288.00
2019-04-09T15:07:36Z	20190409-0052	47	J1056–6258	296.00
2019-04-09T15:15:21Z	20190409-0053	44	J1056–6258	295.40
2019-04-09T15:23:14Z	20190409-0051	50	J1056–6258	288.00
2019-04-09T15:31:09Z	20190409-0054	41	J1056–6258	295.40
2019-04-09T15:38:58Z	20190409-0055	38	J1056–6258	296.00
2019-04-09T15:50:04Z	20190409-0057	32	J1056–6258	288.00
2019-04-09T15:57:43Z	20190409-0068	35	J1056–6258	288.00
2019-04-09T16:06:05Z	20190409-0058	29	J1056–6258	288.00
2019-04-09T16:17:19Z	20190409-0060	23	J1056–6258	288.00
2019-04-09T16:25:00Z	20190409-0069	26	J1056–6258	288.00
2019-04-09T16:33:38Z	20190409-0061	20	J1056–6258	288.00
2019-04-09T16:41:46Z	20190409-0062	17	J1056–6258	288.00
2019-04-09T16:49:41Z	20190409-0063	14	J1056–6258	288.00
2019-04-09T16:58:06Z	20190409-0064	11	J1056–6258	288.00
2019-04-09T17:06:07Z	20190409-0065	8	J1056–6258	288.00
2019-04-09T17:18:16Z	20190409-0070	5	J1056–6258	288.00
2019-04-09T17:25:56Z	20190409-0067	2	J1056–6258	295.48

*Experiment 5*

Start (UTC)	Schedule Block ID	Nants	Target	Duration (sec)
2019-04-29T22:08:50Z	20190429-0051	57	J1056–6258	288.00
2019-04-29T22:16:14Z	20190429-0052	56	J1056–6258	288.00
2019-04-29T22:23:16Z	20190429-0053	53	J1056–6258	288.00
2019-04-29T22:30:14Z	20190429-0056	44	J1056–6258	288.00
2019-04-29T22:37:23Z	20190429-0054	50	J1056–6258	288.00
2019-04-29T22:44:22Z	20190429-0055	47	J1056–6258	288.00

2019-04-29T22:51:16Z	20190429-0059	35	J1056–6258	288.00
2019-04-29T22:58:13Z	20190429-0057	41	J1056–6258	288.00
2019-04-29T23:05:15Z	20190429-0058	38	J1056–6258	288.00
2019-04-29T23:12:19Z	20190429-0061	29	J1056–6258	288.00
2019-04-29T23:19:27Z	20190429-0060	32	J1056–6258	288.00
2019-04-29T23:26:30Z	20190429-0062	26	J1056–6258	288.00
2019-04-29T23:33:29Z	20190429-0063	23	J1056–6258	288.00
2019-04-29T23:40:29Z	20190429-0065	17	J1056–6258	288.00
2019-04-29T23:47:58Z	20190429-0064	20	J1056–6258	288.00
2019-04-29T23:54:56Z	20190429-0067	11	J1056–6258	296.00
2019-04-30T00:01:56Z	20190429-0066	14	J1056–6258	288.00
2019-04-30T00:08:52Z	20190429-0068	8	J1056–6258	288.00
2019-04-30T00:15:55Z	20190429-0069	5	J1056–6258	288.00
2019-04-30T00:22:51Z	20190429-0070	2	J1056–6258	288.00
2019-04-30T00:30:03Z	20190430-0001	23	J1056–6258	288.00
2019-04-30T00:36:59Z	20190430-0002	17	J1056–6258	288.00

#### Experiment 6

Start (UTC)	Schedule Block ID	Nants	Target	Duration (sec)
2019-05-16T17:08:43Z	20190516-0033	60	J1056–6258	288.00
2019-05-16T17:18:14Z	20190516-0034	57	J1056–6258	288.00
2019-05-16T17:25:16Z	20190516-0035	54	J1056–6258	288.00
2019-05-16T17:32:23Z	20190516-0036	51	J1056–6258	288.00
2019-05-16T17:39:23Z	20190516-0037	48	J1056–6258	288.00
2019-05-16T17:46:24Z	20190516-0040	39	J1056–6258	288.00
2019-05-16T17:53:22Z	20190516-0038	45	J1056–6258	288.00
2019-05-16T18:00:29Z	20190516-0039	42	J1056–6258	288.00
2019-05-16T18:07:31Z	20190516-0041	36	J1056–6258	288.00
2019-05-16T18:14:30Z	20190516-0046	21	J1056–6258	296.00
2019-05-16T18:21:28Z	20190516-0042	33	J1056–6258	288.00
2019-05-16T18:28:28Z	20190516-0053	60	J1056–6258	288.00
2019-05-16T18:35:37Z	20190516-0043	30	J1056–6258	288.00
2019-05-16T18:42:35Z	20190516-0044	27	J1056–6258	288.00
2019-05-16T18:49:39Z	20190516-0045	24	J1056–6258	288.00
2019-05-16T18:56:40Z	20190516-0047	18	J1056–6258	288.00
2019-05-16T19:03:48Z	20190516-0048	15	J1056–6258	295.09
2019-05-16T19:10:49Z	20190516-0049	12	J1056–6258	288.00
2019-05-16T19:17:49Z	20190516-0050	9	J1056–6258	288.00
2019-05-16T19:24:52Z	20190516-0051	6	J1056–6258	288.00
2019-05-16T19:31:54Z	20190516-0052	3	J1056–6258	288.00

#### Experiment 7

Start (UTC)	Schedule Block ID	Nants	Target	Duration (sec)
2019-05-16T19:39:01Z	20190516-0054	60	J1644–4559	288.00
2019-05-16T19:46:26Z	20190516-0055	57	J1644–4559	288.00
2019-05-16T19:53:29Z	20190516-0056	54	J1644–4559	295.65
2019-05-16T20:00:30Z	20190516-0057	51	J1644–4559	288.00
2019-05-16T20:07:37Z	20190516-0058	48	J1644–4559	288.00
2019-05-16T20:14:54Z	20190516-0059	45	J1644–4559	288.00
2019-05-16T20:21:57Z	20190516-0060	42	J1644–4559	288.00
2019-05-16T20:29:08Z	20190516-0061	39	J1644–4559	288.00
2019-05-16T20:36:05Z	20190516-0062	36	J1644–4559	288.00
2019-05-16T20:43:01Z	20190516-0063	33	J1644–4559	288.00
2019-05-16T20:50:04Z	20190516-0064	30	J1644–4559	288.00
2019-05-16T20:57:01Z	20190516-0065	27	J1644–4559	288.00
2019-05-16T21:04:06Z	20190516-0066	24	J1644–4559	288.00
2019-05-16T21:11:12Z	20190516-0067	21	J1644–4559	295.13

2019-05-16T21:18:14Z	20190516-0068	18	J1644–4559	288.00
2019-05-16T21:25:19Z	20190516-0069	15	J1644–4559	288.00
2019-05-16T21:32:21Z	20190516-0070	12	J1644–4559	288.00
2019-05-16T21:39:26Z	20190516-0071	9	J1644–4559	288.00
2019-05-16T21:46:29Z	20190516-0072	6	J1644–4559	288.00
2019-05-16T21:53:32Z	20190516-0073	3	J1644–4559	288.00
2019-05-16T22:00:41Z	20190516-0074	60	J1644–4559	295.80

*Experiment 8*

Start (UTC)	Schedule Block ID	Nants	Target	Duration (sec)
2019-06-07T16:29:28Z	20190607-0028	62	J1056–6258	295.76
2019-06-07T16:37:01Z	20190607-0041	23	J1056–6258	296.65
2019-06-07T16:44:05Z	20190607-0029	59	J1056–6258	296.87
2019-06-07T16:51:11Z	20190607-0032	50	J1056–6258	296.80
2019-06-07T16:58:19Z	20190607-0030	56	J1056–6258	296.47
2019-06-07T17:05:26Z	20190607-0031	53	J1056–6258	296.55
2019-06-07T17:12:42Z	20190607-0042	20	J1056–6258	296.80
2019-06-07T17:19:50Z	20190607-0046	8	J1056–6258	296.72
2019-06-07T17:26:59Z	20190607-0043	17	J1056–6258	296.80
2019-06-07T17:34:07Z	20190607-0044	14	J1056–6258	296.94
2019-06-07T17:41:13Z	20190607-0045	11	J1056–6258	296.26
2019-06-07T17:48:14Z	20190607-0047	5	J1056–6258	296.72
2019-06-07T17:55:18Z	20190607-0048	2	J1056–6258	296.01

*Experiment 9*

Start (UTC)	Schedule Block ID	Nants	Target	Duration (sec)
2019-06-08T13:35:37Z	20190608-0003	62	J1056–6258	296.72
2019-06-08T13:48:29Z	20190608-0006	53	J1056–6258	296.65
2019-06-08T13:55:33Z	20190608-0007	50	J1056–6258	296.33
2019-06-08T14:02:38Z	20190608-0008	47	J1056–6258	296.65
2019-06-08T14:09:46Z	20190608-0009	44	J1056–6258	296.40
2019-06-08T14:16:48Z	20190608-0010	41	J1056–6258	296.33
2019-06-08T14:23:51Z	20190608-0012	35	J1056–6258	296.00
2019-06-08T14:31:02Z	20190608-0013	32	J1056–6258	296.55
2019-06-08T14:38:06Z	20190608-0014	29	J1056–6258	296.00
2019-06-08T14:45:13Z	20190608-0015	26	J1056–6258	296.15
2019-06-08T14:52:13Z	20190608-0016	23	J1056–6258	296.55
2019-06-08T14:59:20Z	20190608-0017	20	J1056–6258	296.55
2019-06-08T15:06:23Z	20190608-0022	5	J1056–6258	297.05
2019-06-08T15:13:28Z	20190608-0018	17	J1056–6258	296.47
2019-06-08T15:20:36Z	20190608-0023	2	J1056–6258	296.94
2019-06-08T15:27:52Z	20190608-0011	38	J1056–6258	297.98
2019-06-08T15:35:03Z	20190608-0004	58	J1056–6258	296.15
2019-06-08T15:42:07Z	20190608-0005	55	J1056–6258	297.19

*Experiment 10*

Start (UTC)	Schedule Block ID	Nants	Target	Duration (sec)
2019-06-16T12:46:33Z	20190616-0003	60	J1056–6258	296.55
2019-06-16T12:56:04Z	20190616-0004	57	J1056–6258	296.72
2019-06-16T13:03:06Z	20190616-0008	46	J1056–6258	296.65
2019-06-16T13:10:11Z	20190616-0005	54	J1056–6258	296.47
2019-06-16T13:17:16Z	20190616-0022	6	J1056–6258	296.01
2019-06-16T13:24:25Z	20190616-0006	54	J1056–6258	297.12
2019-06-16T13:31:35Z	20190616-0007	49	J1056–6258	296.00
2019-06-16T13:38:43Z	20190616-0009	43	J1056–6258	296.94
2019-06-16T13:46:02Z	20190616-0010	40	J1056–6258	296.00
2019-06-16T13:53:05Z	20190616-0011	37	J1056–6258	296.08
2019-06-16T14:00:19Z	20190616-0012	35	J1056–6258	296.87
2019-06-16T14:07:27Z	20190616-0013	32	J1056–6258	296.00
2019-06-16T14:14:32Z	20190616-0014	30	J1056–6258	296.72
2019-06-16T14:21:38Z	20190616-0015	27	J1056–6258	298.12
2019-06-16T14:29:12Z	20190616-0016	24	J1056–6258	296.00
2019-06-16T14:36:21Z	20190616-0017	21	J1056–6258	297.12
2019-06-16T14:43:25Z	20190616-0018	18	J1056–6258	297.00
2019-06-16T14:50:33Z	20190616-0019	15	J1056–6258	296.94
2019-06-16T14:57:38Z	20190616-0024	60	J1056–6258	296.55
2019-06-16T15:04:47Z	20190616-0020	12	J1056–6258	296.00
2019-06-16T15:12:00Z	20190616-0021	9	J1056–6258	297.12
2019-06-16T15:19:07Z	20190616-0023	3	J1056–6258	296.47

*Experiment 11*

Start (UTC)	Schedule Block ID	Nants	Target	Duration (sec)
2019-06-17T23:21:01Z	20190617-0040	2	J1644–4559	297.01
2019-06-17T23:28:28Z	20190617-0026	44	J1644–4559	296.28
2019-06-17T23:35:35Z	20190617-0039	5	J1644–4559	296.00
2019-06-17T23:42:38Z	20190617-0038	8	J1644–4559	296.00
2019-06-17T23:49:44Z	20190617-0037	11	J1644–4559	297.23
2019-06-17T23:56:56Z	20190617-0024	50	J1644–4559	296.28
2019-06-18T00:03:57Z	20190617-0036	14	J1644–4559	297.23
2019-06-18T00:11:02Z	20190617-0035	17	J1644–4559	297.00

2019-06-18T00:18:09Z	20190617-0034	20	J1644–4559	296.72
2019-06-18T00:25:11Z	20190617-0033	23	J1644–4559	297.01
2019-06-18T00:39:20Z	20190617-0030	32	J1644–4559	296.72
2019-06-18T00:46:28Z	20190617-0031	29	J1644–4559	297.97
2019-06-18T00:53:35Z	20190617-0029	35	J1644–4559	299.14
2019-06-18T01:00:44Z	20190617-0028	38	J1644–4559	296.57
2019-06-18T01:07:40Z	20190617-0027	41	J1644–4559	296.72
2019-06-18T01:14:50Z	20190617-0025	47	J1644–4559	296.72
2019-06-18T01:21:51Z	20190617-0023	53	J1644–4559	296.00
2019-06-18T01:28:57Z	20190617-0022	56	J1644–4559	296.00
2019-06-18T01:36:03Z	20190617-0021	59	J1644–4559	296.28
2019-06-18T01:44:05Z	20190618-0001	14	J1644–4559	296.28
2019-06-18T01:51:10Z	20190618-0002	32	J1644–4559	296.00

*Experiment 12*

Start (UTC)	Schedule Block ID	Nants	Target	Duration (sec)
2019-07-11T18:36:15Z	20190711-0046	56	J1056–6258	296.00
2019-07-11T18:44:02Z	20190711-0047	53	J1056–6258	296.72
2019-07-11T18:51:15Z	20190711-0048	50	J1056–6258	296.87
2019-07-11T18:58:19Z	20190711-0049	47	J1056–6258	296.94
2019-07-11T19:05:21Z	20190711-0055	29	J1056–6258	296.87
2019-07-11T19:12:21Z	20190711-0050	44	J1056–6258	296.47
2019-07-11T19:18:50Z	20190711-0059	17	J1056–6258	296.26
2019-07-11T19:26:24Z	20190711-0051	41	J1056–6258	296.80
2019-07-11T19:33:22Z	20190711-0060	14	J1056–6258	296.00
2019-07-11T19:40:18Z	20190711-0052	38	J1056–6258	296.33
2019-07-11T19:47:29Z	20190711-0053	35	J1056–6258	297.12
2019-07-11T19:53:53Z	20190711-0054	32	J1056–6258	296.40
2019-07-11T20:01:03Z	20190711-0057	23	J1056–6258	296.55
2019-07-11T20:08:03Z	20190711-0056	26	J1056–6258	296.33
2019-07-11T20:15:05Z	20190711-0061	11	J1056–6258	296.26
2019-07-11T20:22:10Z	20190711-0063	5	J1056–6258	296.47
2019-07-11T20:29:19Z	20190711-0062	8	J1056–6258	296.26
2019-07-11T20:36:22Z	20190711-0064	2	J1056–6258	296.87
2019-07-11T20:43:23Z	20190711-0058	20	J1056–6258	296.47

*Experiment 13*

Start (UTC)	Schedule Block ID	Nants	Target	Duration (sec)
2019-07-21T13:31:52Z	20190721-0016	37	J1056–6258	77.98
2019-07-21T13:39:54Z	20190721-0017	60	J1056–6258	296.47
2019-07-21T13:47:02Z	20190721-0018	58	J1056–6258	298.19
2019-07-21T13:54:06Z	20190721-0023	43	J1056–6258	296.72
2019-07-21T14:01:12Z	20190721-0022	46	J1056–6258	296.55
2019-07-21T14:08:20Z	20190721-0021	49	J1056–6258	296.80
2019-07-21T14:15:23Z	20190721-0020	52	J1056–6258	296.65
2019-07-21T14:22:28Z	20190721-0019	55	J1056–6258	295.94
2019-07-21T14:29:26Z	20190721-0024	40	J1056–6258	296.01
2019-07-21T14:36:43Z	20190721-0025	37	J1056–6258	297.05
2019-07-21T14:43:44Z	20190721-0026	34	J1056–6258	297.58
2019-07-21T14:50:53Z	20190721-0028	28	J1056–6258	297.19
2019-07-21T14:57:57Z	20190721-0027	31	J1056–6258	297.00
2019-07-21T15:05:01Z	20190721-0029	25	J1056–6258	296.00
2019-07-21T15:11:59Z	20190721-0030	22	J1056–6258	296.87
2019-07-21T15:19:11Z	20190721-0037	1	J1056–6258	296.87
2019-07-21T15:26:09Z	20190721-0036	4	J1056–6258	296.94
2019-07-21T15:33:22Z	20190721-0034	10	J1056–6258	296.55
2019-07-21T15:40:20Z	20190721-0035	7	J1056–6258	296.47

2019-07-21T15:47:33Z	20190721-0032	16	J1056–6258	297.00
2019-07-21T15:54:40Z	20190721-0033	13	J1056–6258	297.58
2019-07-21T16:01:34Z	20190721-0031	19	J1056–6258	296.55

*Experiment 14*

Start (UTC)	Schedule Block ID	Nants	Target	Duration (sec)
2019-08-02T18:43:24Z	20190802-0034	5	J1644–4559	298.26
2019-08-02T18:51:06Z	20190802-0033	8	J1644–4559	297.31
2019-08-02T18:58:29Z	20190802-0032	11	J1644–4559	296.00
2019-08-02T19:05:46Z	20190802-0031	14	J1644–4559	297.60
2019-08-02T19:12:51Z	20190802-0026	29	J1644–4559	296.87
2019-08-02T19:19:55Z	20190802-0030	17	J1644–4559	296.57
2019-08-02T19:26:57Z	20190802-0029	20	J1644–4559	296.65
2019-08-02T19:34:01Z	20190802-0028	23	J1644–4559	296.65
2019-08-02T19:41:02Z	20190802-0027	26	J1644–4559	296.87
2019-08-02T19:48:08Z	20190802-0024	35	J1644–4559	296.79
2019-08-02T19:55:12Z	20190802-0025	32	J1644–4559	296.00
2019-08-02T20:02:15Z	20190802-0022	41	J1644–4559	297.16
2019-08-02T20:09:29Z	20190802-0023	38	J1644–4559	296.21
2019-08-02T20:16:38Z	20190802-0021	44	J1644–4559	296.65
2019-08-02T20:23:38Z	20190802-0020	47	J1644–4559	295.91
2019-08-02T20:30:46Z	20190802-0019	50	J1644–4559	296.72
2019-08-02T20:38:07Z	20190802-0018	53	J1644–4559	296.13
2019-08-02T20:45:21Z	20190802-0017	56	J1644–4559	296.65
2019-08-02T20:52:22Z	20190802-0015	58	J1644–4559	296.57
2019-08-02T20:59:29Z	20190802-0016	58	J1644–4559	296.72

*Experiment 15*

Start (UTC)	Schedule Block ID	Nants	Target	Duration (sec)
2019-08-03T08:33:59Z	20190803-0003	58	J1056–6258	296.40
2019-08-03T08:43:28Z	20190803-0004	58	J1056–6258	296.94
2019-08-03T08:50:33Z	20190803-0005	56	J1056–6258	297.05
2019-08-03T08:57:33Z	20190803-0006	53	J1056–6258	297.00
2019-08-03T09:04:39Z	20190803-0007	50	J1056–6258	296.15
2019-08-03T09:11:45Z	20190803-0008	47	J1056–6258	296.94
2019-08-03T09:18:50Z	20190803-0009	44	J1056–6258	296.26
2019-08-03T09:25:55Z	20190803-0010	41	J1056–6258	296.65
2019-08-03T09:32:57Z	20190803-0015	26	J1056–6258	297.19
2019-08-03T09:40:02Z	20190803-0011	38	J1056–6258	296.15
2019-08-03T09:47:06Z	20190803-0016	23	J1056–6258	297.26
2019-08-03T09:54:06Z	20190803-0012	35	J1056–6258	296.40
2019-08-03T10:01:14Z	20190803-0013	32	J1056–6258	296.40
2019-08-03T10:08:22Z	20190803-0014	29	J1056–6258	296.80
2019-08-03T10:15:46Z	20190803-0017	20	J1056–6258	295.87
2019-08-03T10:22:55Z	20190803-0018	17	J1056–6258	296.00
2019-08-03T10:30:04Z	20190803-0019	14	J1056–6258	296.40
2019-08-03T10:37:08Z	20190803-0020	11	J1056–6258	296.33
2019-08-03T10:44:15Z	20190803-0021	8	J1056–6258	297.26
2019-08-03T10:51:24Z	20190803-0022	5	J1056–6258	296.72

*Experiment 16*

Start (UTC)	Schedule Block ID	Nants	Target	Duration (sec)
2019-08-10T08:44:35Z	20190810-0016	43	J1056–6258	298.51
2019-08-10T08:51:59Z	20190810-0011	58	J1056–6258	296.65
2019-08-10T08:59:08Z	20190810-0017	40	J1056–6258	296.55
2019-08-10T09:06:20Z	20190810-0028	7	J1056–6258	296.87

2019-08-10T09:13:27Z	20190810-0030	1	J1056–6258	296.94
2019-08-10T09:20:33Z	20190810-0029	4	J1056–6258	296.87
2019-08-10T09:27:45Z	20190810-0027	10	J1056–6258	297.33
2019-08-10T09:34:51Z	20190810-0026	13	J1056–6258	296.55
2019-08-10T09:41:55Z	20190810-0025	16	J1056–6258	297.91
2019-08-10T09:48:58Z	20190810-0024	19	J1056–6258	297.12
2019-08-10T09:56:03Z	20190810-0023	22	J1056–6258	296.65
2019-08-10T10:03:08Z	20190810-0022	25	J1056–6258	298.44
2019-08-10T10:10:07Z	20190810-0021	28	J1056–6258	296.72
2019-08-10T10:17:26Z	20190810-0020	31	J1056–6258	296.55
2019-08-10T10:24:36Z	20190810-0019	34	J1056–6258	296.80
2019-08-10T10:31:37Z	20190810-0018	37	J1056–6258	296.26
2019-08-10T10:38:42Z	20190810-0015	46	J1056–6258	296.00
2019-08-10T10:45:48Z	20190810-0014	49	J1056–6258	297.40
2019-08-10T10:53:00Z	20190810-0013	52	J1056–6258	297.40
2019-08-10T11:00:10Z	20190810-0012	55	J1056–6258	297.05
2019-08-10T11:07:17Z	20190810-0010	61	J1056–6258	296.87

*Experiment 17*

Start (UTC)	Schedule Block ID	Nants	Target	Duration (sec)
2019-08-13T10:31:27Z	20190813-0017	12	J1056–6258	295.47
2019-08-13T10:38:24Z	20190813-0018	9	J1056–6258	295.69
2019-08-13T10:45:20Z	20190813-0015	18	J1056–6258	295.87

*Experiment 18 (run with single schedule block)*

2019-08-13T09:05:00.081Z	20190813-0023	45	J1056–6258	300.88
2019-08-13T09:10:40.094Z	20190813-0023	42	J1056–6258	300.95
2019-08-13T09:16:20.594Z	20190813-0023	39	J1056–6258	301.67
2019-08-13T09:22:00.758Z	20190813-0023	36	J1056–6258	301.67
2019-08-13T09:27:40.575Z	20190813-0023	33	J1056–6258	301.27
2019-08-13T09:33:20.315Z	20190813-0023	30	J1056–6258	301.41
2019-08-13T09:39:00.721Z	20190813-0023	27	J1056–6258	301.49
2019-08-13T09:44:40.409Z	20190813-0023	24	J1056–6258	301.20
2019-08-13T09:50:20.489Z	20190813-0023	21	J1056–6258	301.27
2019-08-13T09:56:00.589Z	20190813-0023	18	J1056–6258	302.99
2019-08-13T10:01:40.381Z	20190813-0023	15	J1056–6258	301.27
2019-08-13T10:07:20.419Z	20190813-0023	12	J1056–6258	300.81
2019-08-13T10:13:00.493Z	20190813-0023	9	J1056–6258	300.95
2019-08-13T10:18:40.540Z	20190813-0023	6	J1056–6258	301.02
2019-08-13T10:24:20.068Z	20190813-0023	3	J1056–6258	300.63

*Experiment 19 (run with single schedule block)*

Start (UTC)	Schedule Block ID	Nants	Target	Duration (sec)
2019-08-25T11:52:39.622Z	20190825-0003	60	J1056–6258	301.95
2019-08-25T11:58:23.623Z	20190825-0003	57	J1056–6258	301.74
2019-08-25T12:04:03.332Z	20190825-0003	54	J1056–6258	301.20
2019-08-25T12:09:43.760Z	20190825-0003	51	J1056–6258	301.67
2019-08-25T12:15:23.281Z	20190825-0003	48	J1056–6258	301.09
2019-08-25T12:21:03.524Z	20190825-0003	45	J1056–6258	301.41
2019-08-25T12:26:43.328Z	20190825-0003	42	J1056–6258	301.20
2019-08-25T12:32:23.344Z	20190825-0003	39	J1056–6258	301.09
2019-08-25T12:38:03.800Z	20190825-0003	36	J1056–6258	301.59
2019-08-25T12:43:43.407Z	20190825-0003	33	J1056–6258	301.88
2019-08-25T12:49:23.310Z	20190825-0003	30	J1056–6258	302.06
2019-08-25T12:55:03.334Z	20190825-0003	27	J1056–6258	301.59
2019-08-25T13:00:43.385Z	20190825-0003	24	J1056–6258	301.59

2019-08-25T13:06:23.852Z	20190825-0003	21	J1056–6258	302.27
2019-08-25T13:12:03.315Z	20190825-0003	18	J1056–6258	301.41
2019-08-25T13:17:43.554Z	20190825-0003	15	J1056–6258	301.95
2019-08-25T13:23:23.458Z	20190825-0003	12	J1056–6258	301.41
2019-08-25T13:29:03.741Z	20190825-0003	9	J1056–6258	302.13
2019-08-25T13:34:43.374Z	20190825-0003	6	J1056–6258	301.81
2019-08-25T13:40:23.710Z	20190825-0003	3	J1056–6258	302.06
2019-08-25T13:46:03.809Z	20190825-0003	1	J1056–6258	302.20

*Experiment 20 (run with single schedule block)*

Start (UTC)	Schedule Block ID	Nants	Target	Duration (sec)
2019-09-01T11:34:20.060Z	20190901-0005	60	J1056–6258	302.60
2019-09-01T11:39:51.021Z	20190901-0005	57	J1056–6258	301.27
2019-09-01T11:45:21.931Z	20190901-0005	54	J1056–6258	302.35
2019-09-01T11:50:53.480Z	20190901-0005	51	J1056–6258	301.88
2019-09-01T11:56:24.449Z	20190901-0005	48	J1056–6258	302.13
2019-09-01T12:01:55.477Z	20190901-0005	45	J1056–6258	301.49
2019-09-01T12:07:25.340Z	20190901-0005	42	J1056–6258	301.34
2019-09-01T12:12:55.068Z	20190901-0005	39	J1056–6258	300.88
2019-09-01T12:18:24.770Z	20190901-0005	36	J1056–6258	301.95
2019-09-01T12:23:54.840Z	20190901-0005	33	J1056–6258	301.59
2019-09-01T12:29:24.302Z	20190901-0005	30	J1056–6258	301.20
2019-09-01T12:34:53.902Z	20190901-0005	27	J1056–6258	301.81
2019-09-01T12:40:23.998Z	20190901-0005	24	J1056–6258	302.27
2019-09-01T12:45:54.945Z	20190901-0005	21	J1056–6258	302.20
2019-09-01T12:51:25.631Z	20190901-0005	18	J1056–6258	301.67

Label	Date	Phase-up Target	Schedule Block ID
Exp 1	2019-03-20	J0408-6545	20190320-0056
Exp 2	2019-04-03	3C286	20190403-0058
Exp 3	2019-04-04	3C286	20190404-0056
Exp 4	2019-04-09	J0408-6545	20190409-0048
Exp 5	2019-04-29	J1939-6342	20190429-0050
Exp 6	2019-05-16	J0408-6545	20190516-0029
Exp 7	2019-05-16	J0408-6545	20190516-0029
Exp 8	2019-06-07	J0408-6545	20190607-0027
Exp 9	2019-06-08	J0408-6545	20190608-0002
Exp 10	2019-06-16	J0408-6545	20190616-0025
Exp 11	2019-06-17	J1939-6342	20190617-0020
Exp 12	2019-07-11	J1939-6342	20190711-0045
Exp 13	2019-07-21	J0825-5010	20190721-0007
Exp 14	2019-08-02	J1939-6342	20190802-0014
Exp 15	2019-08-03	J0408-6545	20190803-0002
Exp 16	2019-08-10	J0408-6545	20190810-0009
Exp 17	2019-08-13	J0408-6545	20190813-0004
Exp 18	2019-08-13	J0408-6545	20190813-0004
Exp 19	2019-08-25	J0408-6545	20190825-0002
Exp 20	2019-09-01	J0408-6545	20190901-0004

Table 5: Summary of the phase-up schedule blocks and targets associated with the set of experiments run.

## A.2 Associated phase-up information

Table 5 shows the schedule block identifiers and phase-up targets (J0408-6545, J1939-6342, 3C286 or J0825-5010) that were run preceding the coherency experiments of Table 4 to ensure a phased-array.

# Beamformer\_Coherency\_Commissioning\_Tests\_1K\_tosign

Final Audit Report

2021-02-08

Created:	2021-02-02
By:	Carmen Humphreys (carmen@ska.ac.za)
Status:	Signed
Transaction ID:	CBJCHBCAABAAtZmnzulP7n9GIFTea7TKcy9oAfMIQBZT

## "Beamformer\_Coherency\_Commissioning\_Tests\_1K\_tosign" History

-  Document created by Carmen Humphreys (carmen@ska.ac.za)  
2021-02-02 - 12:05:19 PM GMT- IP address: 105.186.96.203
-  Document emailed to Marisa Geyer (mgeyer@ska.ac.za) for signature  
2021-02-02 - 12:26:49 PM GMT
-  Email viewed by Marisa Geyer (mgeyer@ska.ac.za)  
2021-02-02 - 12:37:29 PM GMT- IP address: 66.249.93.117
-  Email viewed by Marisa Geyer (mgeyer@ska.ac.za)  
2021-02-03 - 12:36:59 PM GMT- IP address: 66.249.93.117
-  Document e-signed by Marisa Geyer (mgeyer@ska.ac.za)  
Signature Date: 2021-02-03 - 12:37:34 PM GMT - Time Source: server- IP address: 168.253.73.169
-  Document emailed to Maciej Serylak (m.serylak@skatelescope.org) for signature  
2021-02-03 - 12:37:36 PM GMT
-  Email viewed by Maciej Serylak (m.serylak@skatelescope.org)  
2021-02-06 - 9:11:06 PM GMT- IP address: 85.255.236.181
-  Email viewed by Maciej Serylak (m.serylak@skatelescope.org)  
2021-02-08 - 10:59:57 AM GMT- IP address: 81.152.125.242
-  Document e-signed by Maciej Serylak (m.serylak@skatelescope.org)  
Signature Date: 2021-02-08 - 11:17:27 AM GMT - Time Source: server- IP address: 81.152.125.242
-  Document emailed to Sharmila Goedhart (sharmila@ska.ac.za) for signature  
2021-02-08 - 11:17:29 AM GMT

 Email viewed by Sharmila Goedhart (sharmila@ska.ac.za)

2021-02-08 - 11:24:22 AM GMT- IP address: 66.249.93.209

 Document e-signed by Sharmila Goedhart (sharmila@ska.ac.za)

Signature Date: 2021-02-08 - 11:24:50 AM GMT - Time Source: server- IP address: 169.0.113.192

 Agreement completed.

2021-02-08 - 11:24:50 AM GMT



**Adobe Sign**